PAPER Nr.: 84

HOVER PERFORMANCE CHARACTERISTICS OF A VARIABLE GEOMETRY ROTOR

BY

ABRAHAM I. SHABAN AND BELLUR L. NAGABHUSHAN

SAINT LOUIS UNIVERSITY, PARKS COLLEGE CAMPUS
CAHOKIA, ILLINOIS, USA

TWENTIETH EUROPEAN ROTORCRAFT FORUM
OCTOBER 4 - 7, 1994 AMSTERDAM

Printed by the Technical Highschool Haarlem

1. Abstract

Hover performance characteristics of a variable geometry rotor are investigated by developing and using a blade element model of such a system. Variation in rotor geometry due to extension of the hinge-offset, telescoping the lifting portion of the rotor blade and incorporation of a lifting type deflectable flap on the rotor blade are considered. The effects of these rotor parameters on its hover performance characteristics are evaluated in terms of the corresponding variations in rotor thrust and required shaft horse power. A trade study using Bell 413 helicopter as the baseline design is presented which indicates that nominal thrust of such a fixed geometry rotor in hover condition can be achieved by using a variable geometry rotor that is 17% smaller in radius R and having a 43% R lifting flap, located at 21.7% R along the blade from the hub center and deflected down 6 degrees. The corresponding required shaft horsepower was also found to be 6% lower while the base line rotor tip speed decreased by 17%.

2. Nomenclature

a	=	Slope of lift curve (Blade airfoil), 1/rad.
a_0	=	Speed of sound, ft/sec.
a_f	=	Slope of lift curve (Flap airfoil), 1/rad.
A	=	Area of disc, ft^2
AR	=	Rotor aspect ratio
A_b	=	Total area of blades, ft^2
A_1	=	First lateral harmonic of blade feathering or lateral cyclic pitch, rad.
b	=	Number of blades
B_1	=	First longitudinal coefficient of blade flapping or longitudinal cyclic pitch, rad.
c	=	Chord of blade, ft.
c_f	=	Chord of flap extension, ft.
C	=	Total chord of blade and extension (= $c + c_f$), ft.
C_{br}	=	Blade chord ratio (=c/R)
c_d	=	Coefficient of drag
C_{Di}	=	Induced drag coefficient
C_L	=	Coefficient of lift
$C_{LM=0}$	=	Section lift coefficient
C_P	=	Coefficient of power
C_T	=	Coefficient of thrust
C_r	=	Flap chord ratio ($=c_f/c$)
$\bar{e}$	=	Hinge offset ratio (= e/r)
F.M.	=	Figure of Merit
L	=	Lift, lb
l_b	=	Lifting blade ratio ($=l_b/R$)
l_f	=	Flap length
L_{br}	=	Lifting blade ratio (= l_b/R)
L_{fr}	=	Flap length ratio ($=l_f/R$)
M	=	Mach number
P	=	Power, hp.

Q	=	Torque, ft - lb.
R	=	Blade radius (= $e + l_b$), ft.
r	=	Radius of blade element, ft.
T	=	Thrust, lb.
V_1	=	Induced velocity, ft/sec.
V	=	Total velocity, ft/sec.
V_{tp}	=	Tip velocity, ft/s
x_f	=	Location of flap inboard edge from hinge, ft.
X_{fr}	=	Flap location parameter (=x_f/r)
α	=	Angle of attack, rad.
α_{oL}	=	Angle of attack at zero lift, rad.
θ	=	Blade pitch angle, rad.
θ_1	=	Blade twist angle, rad.
θ_0	=	Collective pitch angle, rad.
θ_t	=	Blade tip pitch angle, rad.
ρ	=	Density of air, slug/ft^3
σ	=	Solidity of rotor
ϕ	=	Inflow angle, rad.
ν	=	Kinematic viscosity, ft^2/sec.
ϕ_t	=	*Induced angle at the tip, rad.*
τ	=	Relative control effectiveness
δ_f	=	Flap deflection, rad.
ψ	=	Azimuth position of blade, rad.
Ω	=	Rotational speed of rotor, rad/sec.
ζ	=	Location of flap inboard edge from hub center (= $e + x_f$), ft.
η	=	Location of flap outboard edge from hub center (= $e + x_f + l_f$)
$(\,)_b$	=	Blade
$(\,)_f$	=	Flap
$(\,)_t$	=	Blade tip

3. Introduction

Improvements in helicopter performance has often resulted in a more complex rotor system. However, a well designed rotor system, albeit sophisticated, need not necessarily degrade the safety and reliability of the vehicle. With this in mind, an attempt is made here to improve helicopter performance by using a variable geometry rotor.

One of the earliest investigations toward the variable geometry rotor was conducted by Sikorsky, which was called TRAC (Telescoping Rotor Aircraft) [Ref. 1, 2]. The project was successfully flight demonstrated, but was canceled due to lack of support and interest. However, flapped rotor blades (servoflap), have already been used for flight control by Kaman SH-2 [Ref. 3, 4]. Studies on advanced rotor control systems [Ref 5-7] and, reliability and maintainability of such systems [Ref. 8] have also been conducted.

In the present case, the performance characteristics of a rotor whose geometry and configuration can be varied by means of a lifting flap and/or blade telescoping will be investigated. Specifically, effects of flap length, flap location on the blade and flap deflection, on rotor performance will be

determined. Also, the concept of telescoping the blade lifting vs nonlifting portions will be considered in varying the rotor geometry. Tradeoff between the rotor blade length and addition of a deflectable lifting flap is of particular interest since a shorter blade radius would lower tip speed, and hence noise, in the hover mode. This can also lead to higher forward speed of the vehicle due to reduced compressibility effects on the shorter blade tips. These aspects are investigated here by initially considering hover performance of such a rotor system. A blade element model of a variable geometry rotor, having the above features, has been developed and used in this study. The following describes the rotor system model, its hover performance characteristics and a trade study which illustrates the performance advantages relative to a conventional rotor.

4. Mathematical Model of Variable Geometry Rotor

The variable geometry rotor model (Figure 1) considered here includes the following features; (a) telescoping the blade by extending the blade lifting surface only, while keeping hinge offset as a constant, or, keeping the lifting blade length as a constant and extending the hinge offset, and (b) use of a high lift device, such as a lifting flap, along the span of the blade with and without flap deflection. To determine the effects of these geometric and flap parameters on the rotor performance, a blade element model was developed to predict thrust and power required in hovering flight.

Rotor Thrust

Based on blade element theory [Ref. 4, 9] total thrust developed by the rotor is given by

$$T = \frac{b}{2\pi}\int_0^{2\pi}\int_0^{R}\frac{\Delta L}{\Delta r}\,dr\,d\psi \qquad (1)$$

The elemental lift variation along the blade can be expressed as

$$\frac{\Delta L}{\Delta r} = \frac{\rho}{2}(\Omega r)^2 a.(\theta - \frac{V_1}{\Omega r})c \qquad (2)$$

where

$$\theta = \theta_0 + \frac{r}{R}\theta_1 - A_1\cos\psi - B_1\sin\psi - \alpha_{OL} \qquad (3)$$

and

$$V_1 = \frac{-\frac{\Omega}{2}acb + \sqrt{(\frac{\Omega}{2}acb)^2 + 8\pi b\Omega^2 r a\theta c}}{8\pi} \qquad (4)$$

The above nonuniform induced velocity model [Ref. 4, 9] was chosen as it reflects variation in flow condition along a geometrically and aerodynamically nonunifrom blade. Also, the blade airfoil is assumed to have camber in defining its pitch angle. For the lifting flap section of the blade the lift coefficient is modelled as

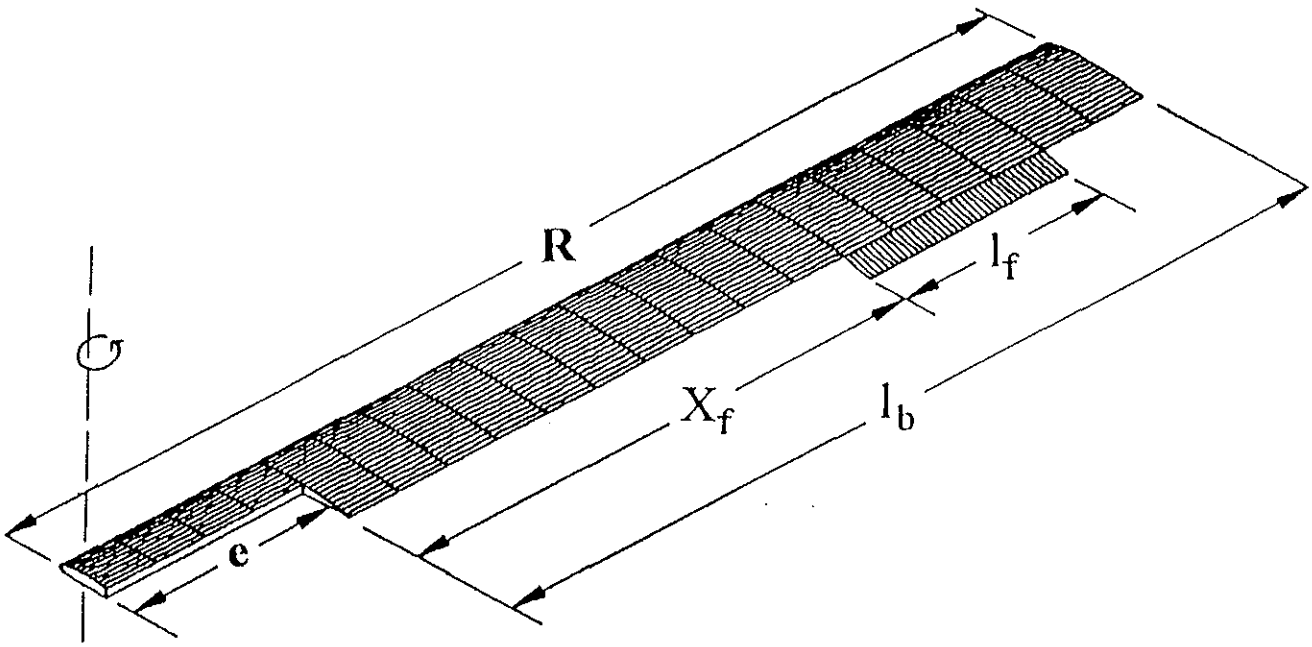

Figure 1. Parameters of variable geometry rotor

$$C_{l_f} = a_f(\alpha_f + \tau\delta_f) \tag{5}$$

where $a_f\ \tau = a_{\delta_f}$ is the lift curve slope of the blade section with deflected flap. The corresponding variation in blade lift along its span is

$$\frac{\Delta L}{\Delta r} = \frac{\rho}{2}(\Omega r)^2\,[\alpha_f + \tau\delta_f]\,a_f\,C \tag{6}$$

Substituting Eqns (2) and (6) into Eqn (1) and assuming the spanwise integration is performed in convenient intervals along the blade to account for geometric variations, the total thrust of the rotor is given by

$$T = \frac{b\rho}{4\pi}\Big[\int_0^{2\pi}\int_0^{e}\Big((\Omega r)^2\,\theta_0 + \frac{\Omega^2 r^3}{R}\,\theta_1 - (\Omega r)^2\,A_1\cos\psi$$

$$- (\Omega r)^2\,B_1\sin\psi - (\Omega r)^2\,\alpha_{0_L}\Big)\,c\,a\,dr\,d\psi$$

$$- \int_0^{2\pi}\int_0^{e}(V_1\,\Omega r)\,c\,a\,dr\,d\psi$$

$$+\int_0^{2\pi}\int_e^{\zeta}\Big((\Omega r)^2\,\theta_0 + \frac{\Omega^2 r^3}{R}\,\theta_1 - (\Omega r)^2\,A_1\cos\psi$$

$$- (\Omega r)^2\,B_1\sin\psi - (\Omega r)^2\,\alpha_{0_L}\Big)\,c\,a\,dr\,d\psi \; - \int_0^{2\pi}\int_e^{\zeta}(V_1\,\Omega r)\,c\,a\,dr\,d\psi$$

$$+\int_0^{2\pi}\int_{\varsigma}^{\eta} [((\Omega r)^2\,\theta_0 + \frac{\Omega^2 r^3}{R}\,\theta_1 - (\Omega r)^2\,A_1\cos\psi$$

$$- (\Omega r)^2\,B_1\sin\psi - (\Omega r)^2\,\alpha_{0_L}) + (\Omega r)^2\,\tau\,\delta_f]\,a_f C\,dr\,d\psi$$

$$-\int_0^{2\pi}\int_{\zeta}^{\eta} (V_1\,\Omega r)\,a_f C\,dr\,d\psi$$

$$+\int_0^{2\pi}\int_{\eta}^{R} ((\Omega r)^2\,\theta_0 + \frac{\Omega^2 r^3}{R}\,\theta_1 - (\Omega r)^2\,A_1\cos\psi$$

$$- (\Omega r)^2\,B_1\sin\psi - (\Omega r)^2\,\alpha_{0_L})\,c\,a\,dr\,d\psi - \int_0^{2\pi}\int_{\eta}^{R} (V_1\,\Omega r)\,c\,a\,dr\,d\psi]$$

In integrating the above equation, the blade was assumed to be nonlifting from the hub center to the hinge axis. Performing closed form integration over the rotor azimuth angle and along the span to the extent possible a more convenient form of the above equation was obtained as

$$T = \frac{b\,\rho}{2}\,[\,(\frac{\Omega^2}{3}\,\theta_0\,(\zeta^3 + R^3 - \eta^3) + \frac{\Omega^2}{4R}\,\theta_1$$

$$(\zeta^4 + R^4 - \eta^4) - \frac{\Omega^2}{3}\,\alpha_{0_L}\,(\zeta^3 + R^3 - \eta^3))\,c\,a$$

$$-\frac{1}{2\pi}\,(\int_0^{2\pi}\int_0^{e} X\,c\,a\,dr\,d\psi + \int_0^{2\pi}\int_e^{\zeta} X\,c\,a\,dr\,d\psi + \int_0^{2\pi}\int_{\eta}^{R} X\,c\,a\,dr\,d\psi)$$

$$+[\,\frac{\Omega^2}{3}\,\theta_0\,(\eta^3 - \zeta^3) + \frac{\Omega^2}{4R}\,\theta_1\,(\eta^4 - \zeta^4)$$

$$-\frac{\Omega^2}{3}\,\alpha_{0_L}\,(\eta^3 - \zeta^3)) + \frac{(\Omega^2)}{3}\,\tau\,\delta_f\,(\eta^3 - \zeta^3)\,a_f C$$

$$-\frac{1}{2\pi}\int_0^{2\pi}\int_{\zeta}^{\eta} X_f\,a_f C\,dr\,d\psi] \qquad (7)$$

where $X = V_1\,\Omega\,r$ is the induced velocity parameter along the blade. This equation was numerically integrated subsequently in determining rotor hover performance.

Rotor Torque

Rotor torque in hover can be expressed using blade element theory [Ref. 4, 9] as

$$Q = \frac{b}{2\pi}\int_0^{2\pi}\int_0^R \frac{\Delta Q}{\Delta r}\, dr.\, d\psi \tag{8}$$

Representing elemental torque as

$$\Delta Q = r\,(\Delta L.\,\phi + \Delta D) \tag{9}$$

where $\Delta D = \frac{\rho}{2}(\Omega r)^2\, c_d\, c.\Delta r$ and $\phi = \frac{V_1}{\Omega r}$

Substituting for elemental lift ΔL from Eqn. (2) into (9) and rewriting Eqn. (8),

$$Q = \frac{b\,\rho\,\Omega^2}{4\pi}\int_0^{2\pi}\int_0^R [r^3\, c\, a\,(\frac{V_1}{\Omega r})(\theta_0 + \frac{r}{R}\theta_1 - A_1\cos\psi$$

$$-B_1\sin\psi - \alpha_{0L} - \frac{V_1}{\Omega r}) + r^3 c_d\, c]\, dr\, d\psi \tag{10}$$

Again, performing the spanwise integration in convenient intervals and accounting for the variations in geometry and lift coefficient along the blade span, Eqn. (10) becomes

$$Q = \frac{b\,\rho\,\Omega^2}{4\pi}[\int_0^{2\pi}\int_0^e [\,ac\,(\frac{V_1}{\Omega r})(r^3\,\theta_0 + \frac{r^4}{R}\theta_1 - r^3\,A_1\cos\psi$$

$$- r^3 B_1\sin\psi - r^3\,\alpha_{0L} - r^3\,(\frac{V_1}{\Omega r})) + r^3\, c_d\, c]\, dr\, d\psi$$

$$+\int_0^{2\pi}\int_e^{\zeta} [ac\,(\frac{V_1}{\Omega r})(r^3\,\theta_0 + \frac{r^4}{R}\theta_1 - r^3\,A_1\cos\psi$$

$$- r^3 B_1\sin\psi - r^3\,\alpha_{0L} - r^3\,(\frac{V_1}{\Omega r})) + r^3\, c_d\, c]\, dr\, d\psi$$

$$+\int_0^{2\pi}\int_{\zeta}^{\eta} [a_f C\,(\frac{V_{1f}}{\Omega r})(r^3\,\theta_0 + \frac{r^4}{R}\theta_1 - r^3\,A_1\cos\psi$$

$$- r^3 B_1\sin\psi - r^3\,\alpha_{0L} - r^3\,(\frac{V_{1f}}{\Omega r}))$$

$$+ a_f\,\tau\,\delta_f\, C\, r^3(\frac{V_{1f}}{\Omega r}) + r^3\, C_{d_f} C]\, dr\, d\psi$$

$$+ \int_0^{2\pi} \int_{\eta}^{R} [ac\,(\frac{V_i}{\Omega r})\,(r^3\,\theta_0 + \frac{r^4}{R}\,\theta_1 - r^3\,A_1\cos\psi$$

$$- r^3 B_1 \sin\psi - r^3\,\alpha_{0_L} - r^3\,(\frac{V_i}{\Omega r})) + r^3\,c_d\,c]\,dr\,d\psi \qquad (11)$$

The corresponding horsepower required in hovering has been determined from Eqn. (12)

$$P = \frac{Q\Omega}{550} \qquad (12)$$

Eqns. (6), (11) and (12) were computed numerically to obtain performance data presented here next.

5. Hover Performance Characteristics

In order to describe the hover performance of a variable geometry rotor, a baseline rotor system (Table 1) is chosen for convenience. This rotor system is fully articulated and represents current state of design technology. Accordingly, the results of varying rotor geometry on its performance are described as changes in thrust and required power from the nominal conditions of this baseline rotor system. The performance characteristics discussed here are assumed to be at mean sea level on a standard day.

Parametric Analysis

Extension of the hinge offset, while keeping constant lifting blade length, was found to increase rotor thrust as well as required power (Figure 2). Typically, increasing hinge offset ratio to 5% from the nominal 2.5% produced a thrust increment of 15% at the expense of a power increment of 12% and a tip speed increase of 2.5%.

Reducing the blade length, for a given hinge offset ratio, tends to reduce both thrust and power required to hover. This reduction of thrust can be compensated by extending the hinge offset to some extent, until the tip speed limit is reached. As illustrated in Figure 3, a 10% reduction in lifting blade length requires an increase of the hinge offset ratio by 17.5% to achieve the nominal thrust and power condition. Clearly, these variations in rotor geometry alone cannot produce an improvement in the rotor performance unless the aerodynamic properties of the rotor blade can be modified.

The effect of using a lifting flap along the rotor blade on the rotor performance is considered next. Basically, use of a high lift device, such as a flap, produces greater rotor lift, similar to flap deflection on a fixed wing of an airplane. In this regard, the proposed lifting flap on the rotor is intended to be deployed and operated in hover mode only, similar to use of flap at low speed approach and landing of an airplane. The rotor flap parameters considered here include flap size, location on the blade and flap deflection angle.

Table 1. Nominal helicopter data

Weights:	
Empty	2,946 kg (6,495 lb)
Max T-O and landing	5,397 kg (11,900 lb)
Transmission Rating:	
T-O	1,044 kw (1,400 shp)
Max Continuous	846 kw (1,134 shp)
Engines:	
Number	2
Maximum T-O Rating	1,342 kw (1,800 shp)
Maximum Usable Power	1,044 kw (1,400 shp)
Rotor Radius	14.02 m (23 ft 0 in)
Chord	0.381 m (1.25 ft)
No. of Blades	4
Tip Speed	237.7 m/s (780 ft/s)
Twist θ_1	-15.5 deg
Collective Range θ_0	0 to 16 deg
Hinge offset ratio (e/R)	0.025
Airfoil (Wortmann)	FX71-H-080
Angle of Attack at Zero Lift α_{0_L}	-3.78 deg
Slop of lift curve a	2 π per rad

Increasing flap length or chord was found (Figures 4 and 5) to increase both thrust and required power in hover. These increases were significantly greater if the flap was also deflected down. Locating an undeflected flap closer to the blade tip produced the same thrust and power increments as a deflected flap closer to the hub. As shown in Figure 6, deploying an undeflected, 0.323R flap at 0.6R on the blade produced a 12% thrust increment while requiring a 35% power increment. The same thrust increment could also be achieved by locating the same flap at 0.1R but deflecting it down 6 degrees and allowing a power increment of 12%.

The effect of flap deflection on thrust and power changes have been found to be almost linear (Figure 7) for small angles of deflection up to 6 degrees. These results suggest that deployment of a lifting flap on the blades can significantly alter the rotor thrust and power required characteristics in hover. Next, use of this variation in rotor configuration to improve the performance of the baseline rotor system in considered.

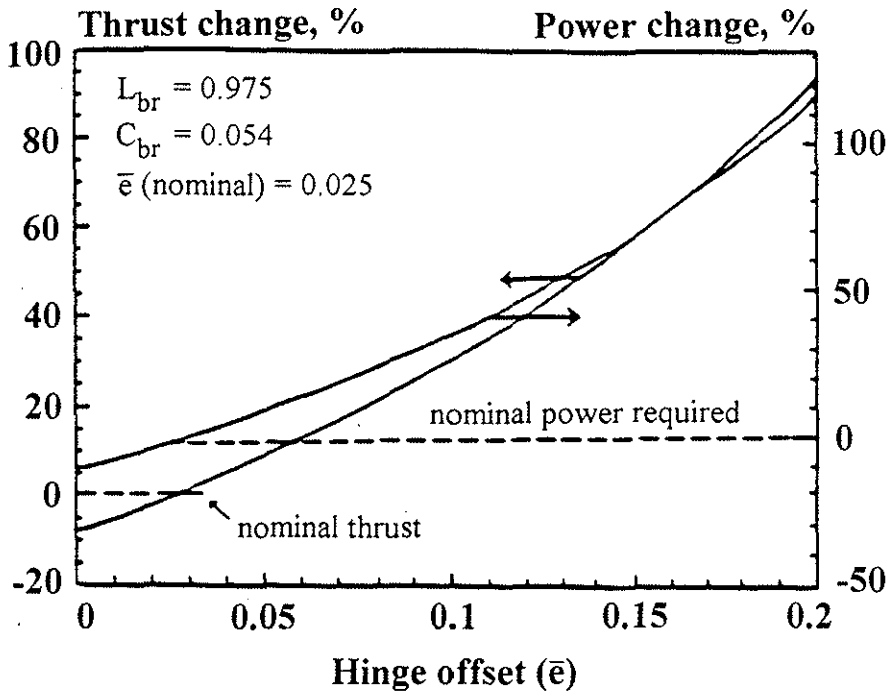

Figure 2. **Hinge offset effect on nominal thrust and power required to hover**

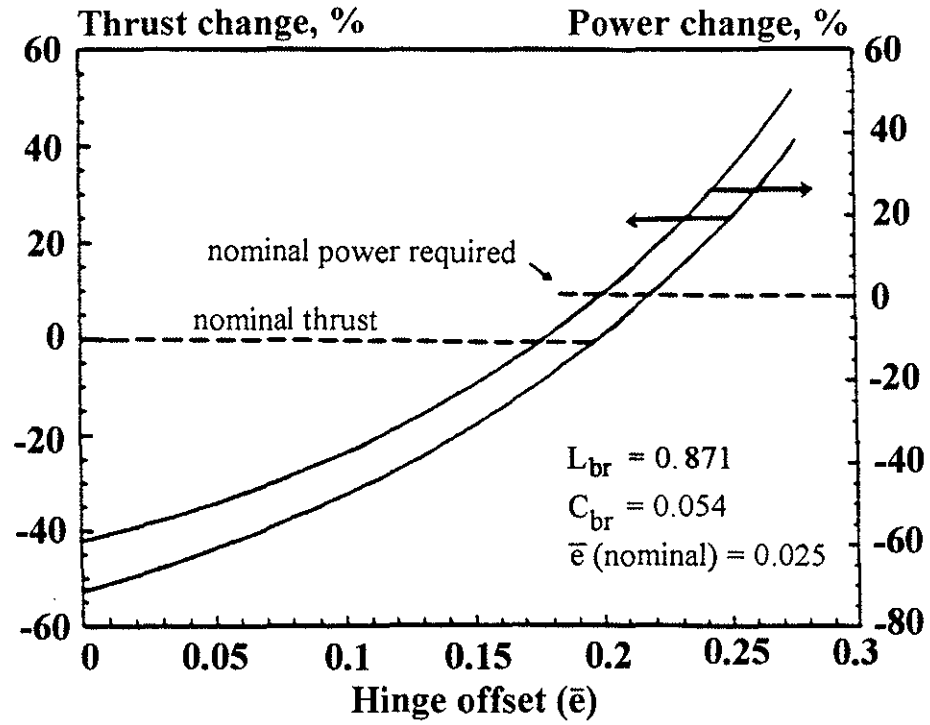

Figure 3. **Effect of reduced blade length on nominal thrust and power required to hover**

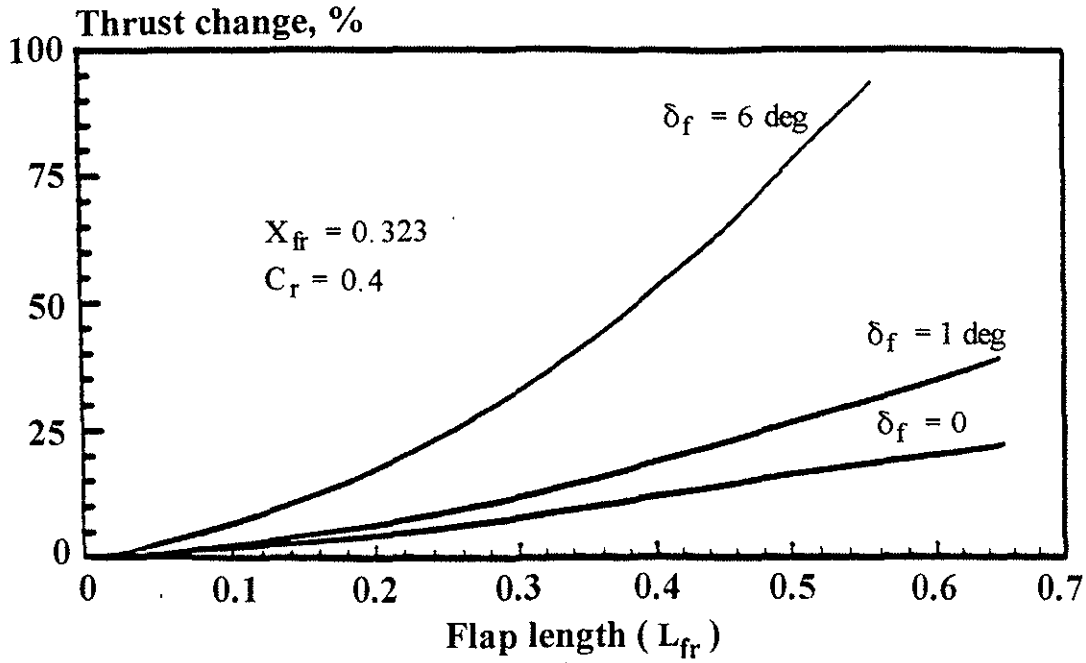

(a)

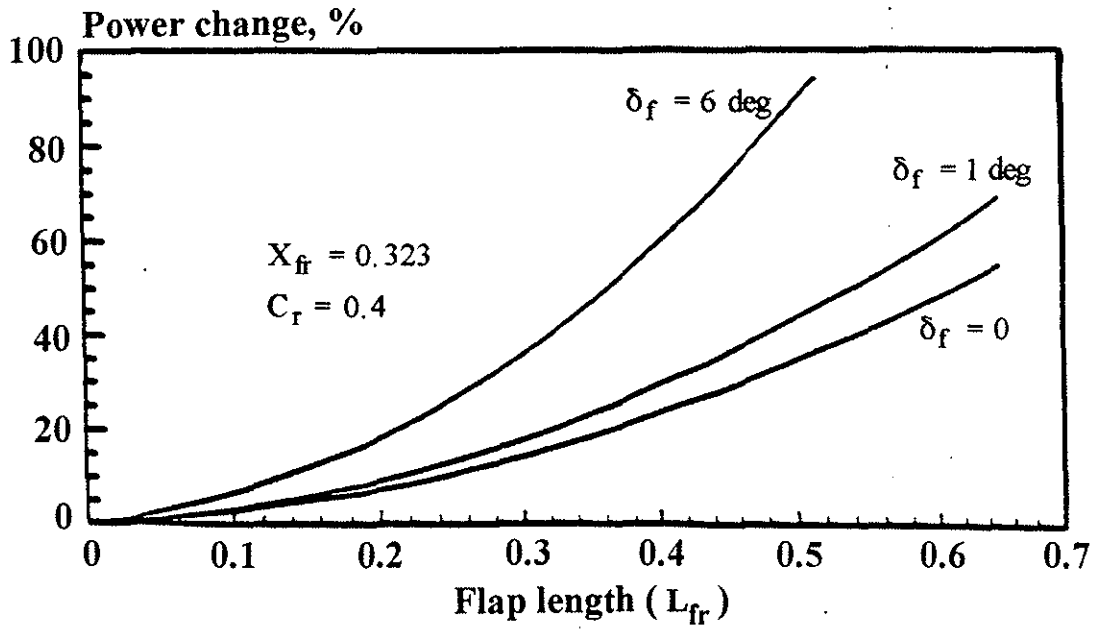

(b)

Figure 4. Flap length effect on nominal thrust and required power

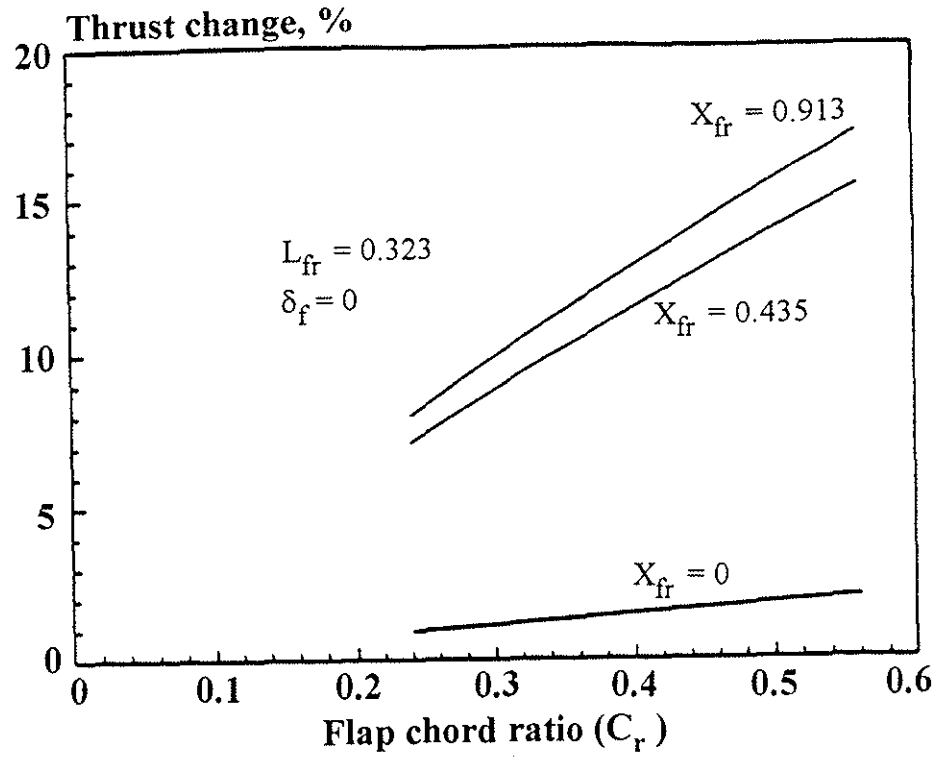

(a)

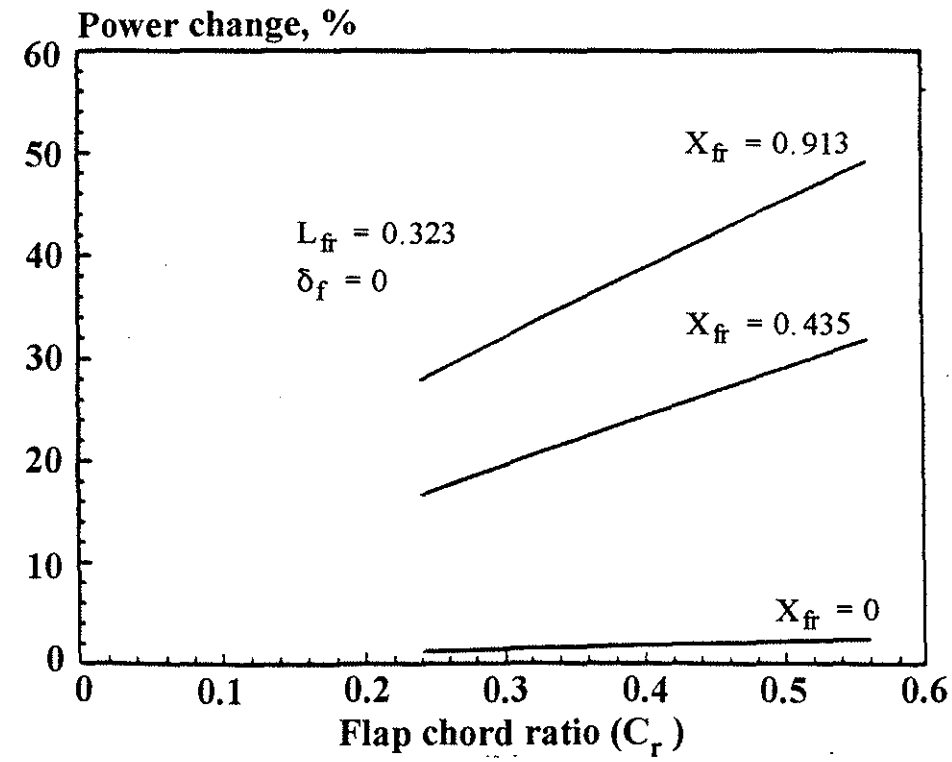

(b)

Figure 5. Flap chord effect on nominal thrust and required power

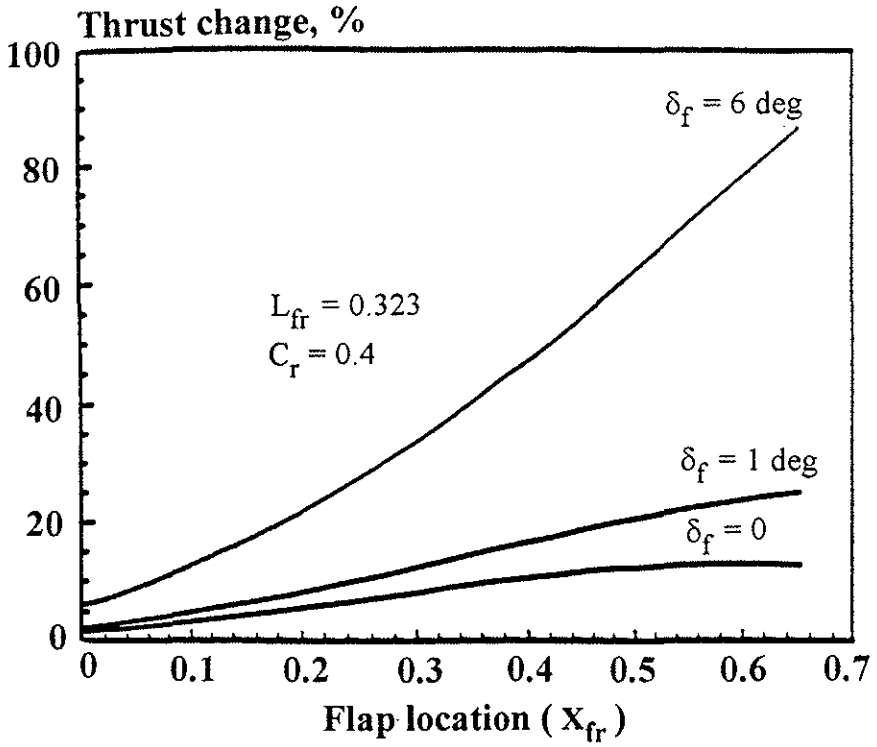

(a)

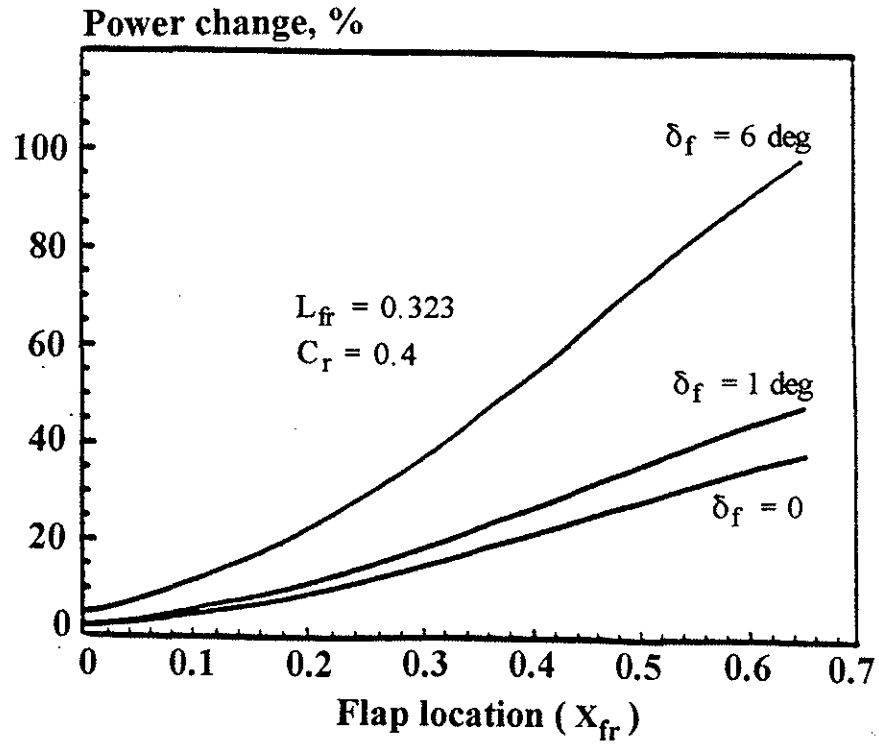

(b)

Figure 6. Flap location effect on nominal thrust and required power

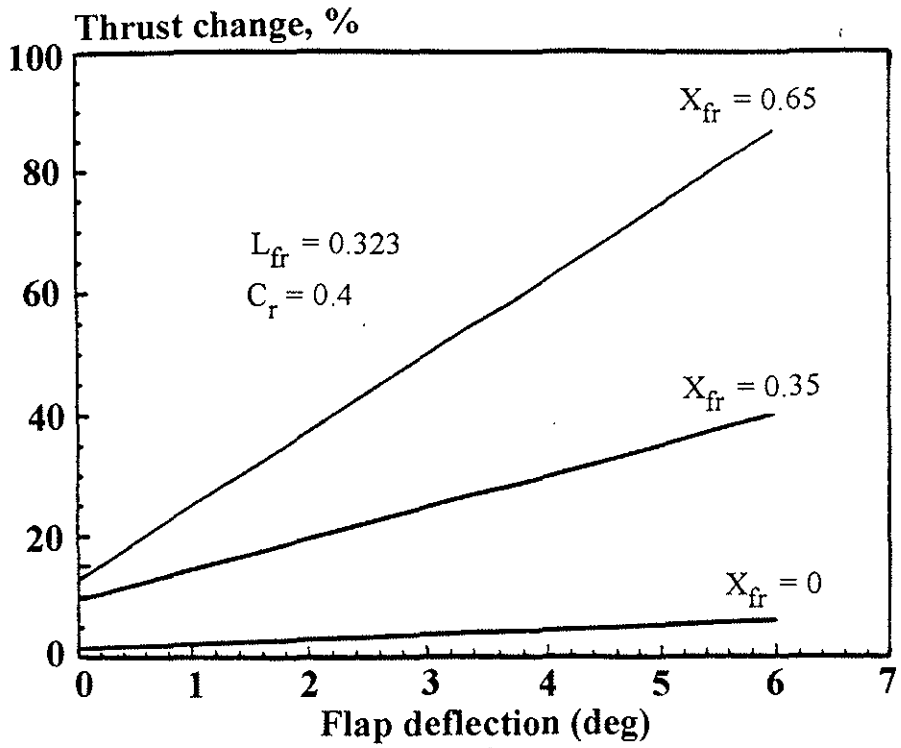

(a)

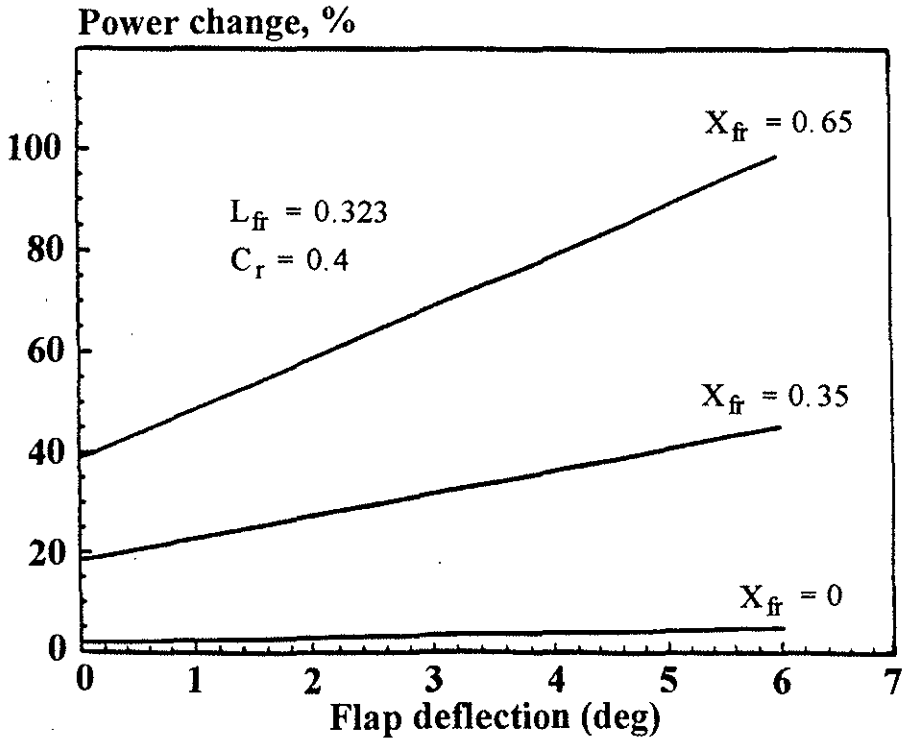

(b)

Figure 7. Flap deflection effect on nominal thrust and required power

Rotor Geometry and Performance Trade

Several flap sizes and locations were selected and consequent results were analyzed with the intent of improving the performance of the baseline rotor system. Also, achieving the same or nominal hover performance but with a reconfigured rotor system was systematically investigated. It was found that locating a 0.39R flap, deflected 6 degrees down, at a location of 0.515R on the blade resulted in nominal thrust of the baseline rotor system (Figure 8). The corresponding power required to hover was found to be 5% less than its nominal value. Alternately, at the nominal power level locating the same flap at 0.58R location was found to produce 8% more than nominal thrust. Use of a longer flap was found to allow locating it more inboard while producing nominal thrust. Consequently, it is observed that rotor geometric configuration can be favorably traded for performance improvement in terms of higher thrust level or lower required power during hover.

Since a shorter blade length is desirable as it permits operation at lower tip speed and hence noise level, it is now intended to trade the blade length for addition of a lifting flap while achieving the nominal rotor system performance. Following several design trades and analysis in this regard, it was found that incorporating a 0.435R flap at a 0.217R location along the blade can generate significant thrust increment depending upon the flap deflection (Figure 9). Typically, with a flap

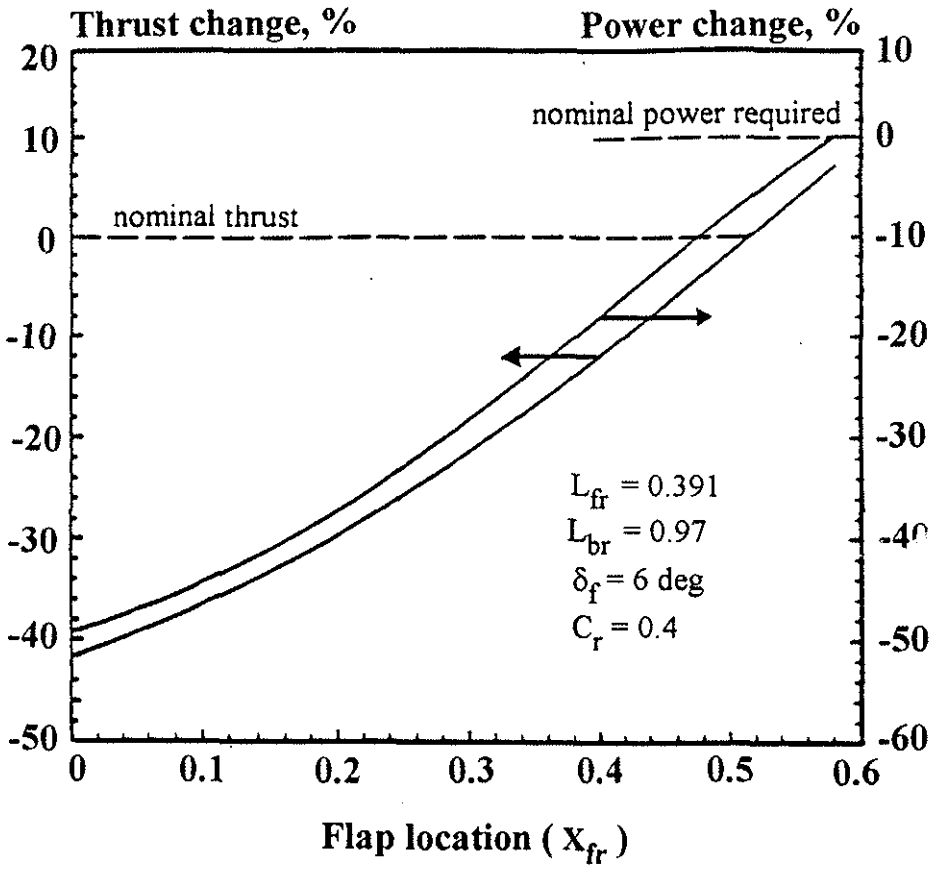

Figure 8. **Combined effect of flap deflection and location on nominal thrust and required power**

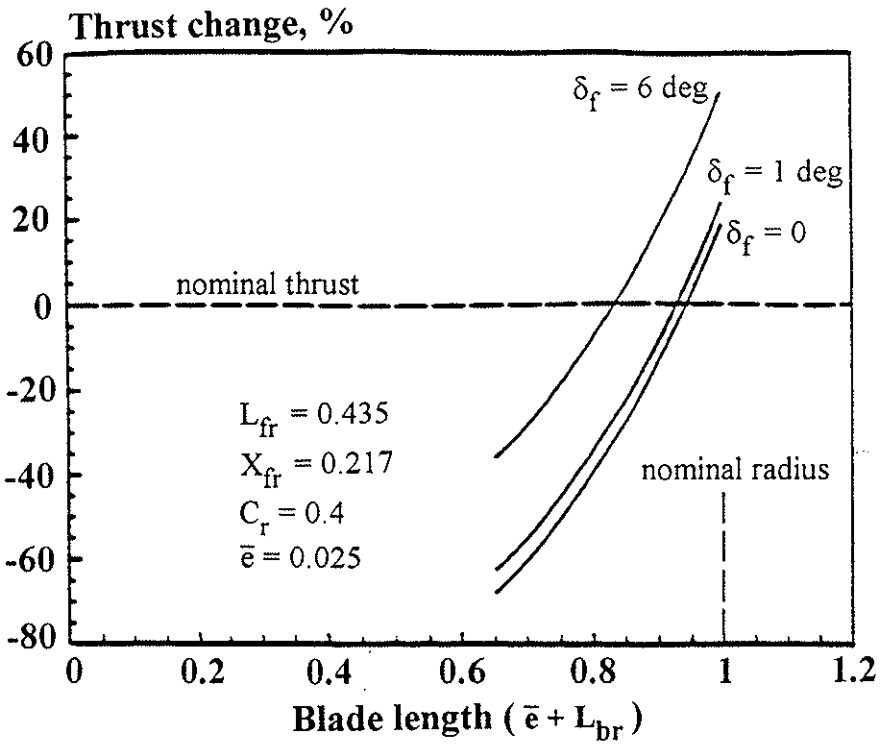

(a)

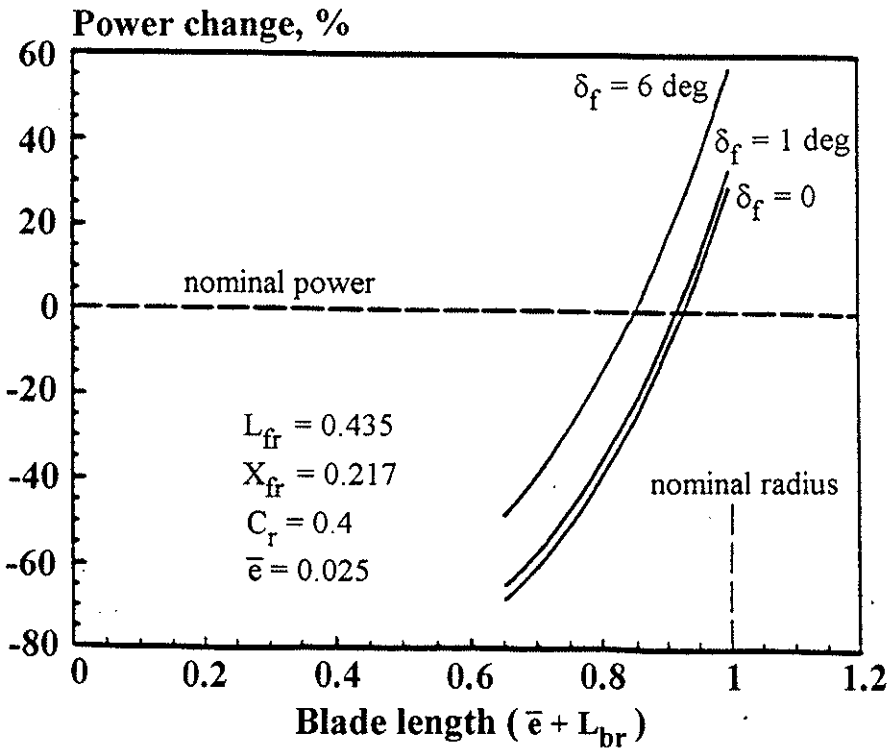

(b)

Figure 9. **Blade length effect on nominal thrust and required power while using a flap**

deployed at 6 degree deflection, a blade radius of 83% of the baseline rotor was found adequate to produce the nominal thrust at 6% lower power than the baseline rotor system. The corresponding tip speed was found to be 17% less than that of the nominal rotor. This can be understood by noting that the solidity ratio of the smaller rotor configuration is increased by 45% while its figure of merit is increased by 8% by the addition of flaps. These results indicate that the rotor blade radius can be decreased by incorporating a deployable lifting flap along the blade, in a given rotor system producing a specified thrust in hover.

6. Concluding Remarks

Varying the rotor geometry and its configuration by changing the hinge-offset distance, lifting blade length and by inclusion of a high lift device such as a flap along the blade have been found to significantly affect the rotor thrust and power requirement in hover. Use of a deflectable flap on the rotor blade was found to yield a more favorable performance improvement than extending or retracting the rotor blades. The latter approach has the added penalty of higher tip speed with blade extension. It was found that the required blade length of a conventionally designed rotor system can be reduced by addition of a lifting flap at an appropriate location on the blade, to produce the specified thrust in hover while requiring less or same level of power input. This has significant implications since it would result in a smaller rotor system having lower noise level as well. Also, such a rotor could achieve higher forward speeds before encountering compressibility effects at the blade tip. It is observed that these performance improvements would be at the expense of a more complex design and operation of the rotor system. These aspects need further investigation before the variable geometry rotor concept can be implemented.

7. Acknowledgments

The authors wish to acknowledge valuable discussions and suggestions provided by Drs. R. M. Andres, S. Karunamoorthy, S. Ahmed and J. A. George during the course of this work.

8. References

1. Fradenburgh, Evan A., "The Variable-Diameter Rotor- A Key to High Performance Rotorcraft," Vertiflite, Vol. 36 March/April, 1990, pp. 46-53.

2. Fradenburgh, Evan A., "Improving Tilt Rotor Aircraft Performance With Variable-Diameter Rotors," Associazione Industrie Aerospazial. Associazione Italiana Di Aeronautica Ed Astronautica. Fourteen European Rotorcraft Forum. Paper No. 30. Milano, Italy, 1988.

3. Gessow, Alferd and Myers, Garry C. Jr., Aerodynamics of the Helicopter, 8th. ed., Gessow and Myers, 1985.

4. Johnson, Wayne, Helicopter Theory, Princeton University Press, Princeton, NJ, 1980.

5. Lemnios, Andrew Z. and Jones, Robert, "The Servo Flap-An Advanced Rotor Control System," American Helicopter Society, Design Specialists' Meeting on Vertical Aircraft Design, San Francisco, California, January 1990.

6. Phillips, Nolan B. and Merkley, Donald J., "BHTI'S Technical Assessment of Advanced Rotor and Control Concepts," American Helicopter Society. Design Specialists' Meeting in Vertical Lift Aircraft Design, San Francisco, California, January, 1990.

7. Straub, Friedrich K. and Merkley, Donald J., "MDHC Technical Assessment of Advanced Rotor and Control Concepts," American Helicopter Society, Design Specialist Meeting on Vertical Lift Aircraft Design, San Francisco, California, January 1990.

8. Hall, Robert A. and Garganese, Ugo S. Jr., "Reliability and Maintainability Evaluation of Rotor Systems, "American Helicopter Society, Annual Forum 37th., New Orleans, LA., 1981, pp. 478-483.

9. Prouty, Raymond W., Helicopter Performance, Stability, and Control, PWS Engineering, Boston, MA, 1986.